

Onset of universality in the dynamical mixing of a pure state

M. Carrera-Núñez¹, A. M. Martínez-Argüello^{2,*}, J. M. Torres³, and E. J. Torres-Herrera³

¹Departamento de Física, Universidad Autónoma Metropolitana-Iztapalapa, Apartado Postal 55-534, 09240 Ciudad de Mexico, Mexico

²Instituto de Ciencias Físicas, Universidad Nacional Autónoma de México, Apartado Postal 48-3, 62210, Cuernavaca, Morelos, Mexico

³Instituto de Física, Benemérita Universidad Autónoma de Puebla, Apartado Postal J-48, Puebla 72570, Mexico

*alael@icf.unam.mx

ABSTRACT

We study the time dynamics of random density matrices generated by evolving the same pure state using a Gaussian orthogonal ensemble (GOE) of Hamiltonians. We show that the spectral statistics of the resulting mixed state is well described by random matrix theory (RMT) and undergoes a crossover from the Gaussian orthogonal ensemble to the Gaussian unitary ensemble (GUE) for short and large times, respectively. Using a semi-analytical treatment relying on a power series of the density matrix as a function of time, we find that the crossover occurs in a characteristic time that scales as the inverse of the dimension. The RMT results are contrasted with a paradigmatic model of many-body localization in the chaotic regime, where the GUE statistics is reached at large times, while for short times the statistics strongly depends on the peculiarity of the considered subspace.

1 Introduction

Random quantum states appear quite naturally in many problems of quantum mechanics. In quantum information theory, for instance, they are indispensable to study the average degree of entanglement in systems where no analytical solution is available^{1,2}. Applications are also found in the theory of open quantum systems, where the effects of a noisy interaction invariably lead to a dynamically generated random state^{3,4}. It is in this context that interesting recent developments have been achieved, where attention has been given to characterize the ensemble of mixed random states inspired in the results of random matrix theory (RMT)⁴⁻⁷. For instance, the eigenvalues of mixed random states belonging to the Hilbert-Schmidt ensemble follow a Marchenko-Pastur distribution^{2,3,8-10}.

An interesting phenomenon appearing in RMT is the transition in the spectral statistics from the Gaussian orthogonal ensemble (GOE) to the Gaussian unitary ensemble (GUE) obtained from varying a single parameter in the Hamiltonian¹¹⁻¹⁴. This phenomenon has been experimentally verified^{15,16}, and it has also been predicted in physical scenarios involving driven non-integrable quantum systems^{17,18}. An interesting question is whether this effect is also present in the case of mixed random states. A random density matrix can be obtained as an incoherent mixture of random pure states, that in turn can be obtained by a random evolution of a fixed initial state. For large times, it is known that such a state belongs to a Wishart ensemble and some spectral properties typically correspond to the GUE³. One can expect, however, that the way such a density matrix is reached as the evolution develops can display interesting features before a universal regime is attained.

In this work we focus on the transient behavior of quantum states before reaching the final random state following the universal GUE statistics. We show that a generic crossover exists for a time scale that depends on the system size. Starting from GOE, the spectral statistics of the state transits in a smooth way to GUE, a transition that is equivalent to that occurring in the spectral statistics of the Hamiltonian when time-reversal symmetry is broken¹⁹⁻²¹. Here, however, the transition is not related to the breaking of anti-unitary symmetries in the Hamiltonian, but with the elements of the density matrix, i.e., real or complex uncorrelated Gaussian random variables. We analyze this behavior using a semi-analytical treatment for the short-time density matrix. Furthermore, we show that the transient behavior to the GUE universal form is also preserved in more realistic situations. For this purpose, we consider that the time evolution of the density matrix is generated by an ensemble of Hamiltonians describing nearest-neighbor interacting spin-1/2 particles with on-site disorder, in the chaotic regime. In this case, the transition to the GUE statistics is also reached for large enough times, while for short times the statistics shows a strong dependence on the peculiarity of the considered subspace.

The paper is organized as follows. In Sec. 2, we explain the dynamical approach that we use to generate random mixed

states. Sec. 3 is devoted to show that a crossover from a GOE-like to a GUE-like statistics in the time-dependent density matrices is possible during the evolution generated by Hamiltonians taken from the GOE. A detailed numerical analysis of the mixed state spectral statistics is given in Sec. 4. We revisit the problem when the evolution is governed by spin-1/2 Hamiltonians in Sec. 5. We show that a transition in the statistical properties is also present for two different subspaces with one of them displaying short-range interactions. Conclusions and final remarks are given in Sec. 6.

2 Ensemble of density matrices

In this section we present a simple model consisting of an ensemble of quantum systems initially prepared in the same state $|\Psi_0\rangle$ and evolving under the influence of a different Hamiltonian. We assume a finite dimensional system, so that the initial state of each member of the ensemble can be represented by a state vector in a Hilbert space of dimension N . The dynamics of the l -th particle is governed by a random Hamiltonian H_l belonging to an ensemble that will be later specified. The time-dependent state vector of each quantum system can be expressed as ($\hbar = 1$)

$$|\Psi_l(t)\rangle = e^{-iH_l t} |\Psi_0\rangle. \quad (1)$$

Using the pure-state evolution generated by each Hamiltonian, equation (1), one can find that the state of the whole ensemble of N pure states is described by their incoherent sum and is given by the following density matrix

$$\rho(t) = \frac{1}{N} \sum_{l=1}^N |\Psi_l(t)\rangle \langle \Psi_l(t)|. \quad (2)$$

A density matrix constructed in this way could, for instance, correspond to N particles initially prepared in the same state, but each one subjected to a different Hamiltonian evolution. In general, however, one could think of N identical quantum systems starting from the same condition, but evolving in different ways. In this work, we restrict ourselves to the case where the number of quantum systems matches the dimension of each separate Hilbert space.

We will focus our attention on Hamiltonians with real entries in certain basis and initial states with random real probability amplitudes in that same basis. In particular, we will start considering each H_l as a member of the GOE. For arbitrary values of time, the mixed state in equation (2) will be given by a density matrix with complex entries. For large enough values of time, it is plausible to infer that real and imaginary parts will have, on average, the same weight. Invoking the central limit theorem (CLT), it is not hard to realize that the resulting density matrix will share some properties with members of the GUE. However, this is not the case for short times. Indeed if one takes the incoherent sum of real random states, the resulting density matrix will resemble a member of the GOE. Numerical evaluation of spectral quantities demonstrates this fact as we will see later in this work, even when each H_l is not a member of the GOE but includes certain random components. For now, let us connect this behavior with previous results involving a crossover from the GOE to the GUE statistics in RMT.

3 GOE to GUE crossover: Onset of universality

It is known that a GOE to GUE statistics crossover can be observed by tuning a parameter in a Hamiltonian of the form

$$H = S + i\alpha A \quad (3)$$

with S a real symmetric Gaussian matrix, and A a real antisymmetric Gaussian matrix having variances

$$\langle (S_{n,n})^2 \rangle = 2\langle (S_{n,m \neq n})^2 \rangle = 2\langle (A_{n,m \neq n})^2 \rangle = 1. \quad (4)$$

In previous works it has been observed that, for a given dimension of the system N , the transition takes place at $\alpha \sim 1/\sqrt{N}$ ^{12,22,23}. Using this result, we will elucidate how a similar crossover arises in time for the simple model of the random density matrix explained above. Furthermore, we will show that at the stage when the GUE statistics is achieved, all other features of a random density matrix are attained as well. It is in this sense that, in this case, the GOE to GUE crossover marks a prelude to the universal feature of a dynamically generated density matrix that we refer to as onset of universality.

3.1 Short-time dynamics

In order to study the aforementioned transition, we consider the short-time behavior of the density matrix by evaluating its expansion as a power series of the time parameter t . For this purpose, we consider the following form of the evolution operator

$$U_l(t) = 1 - itH_l - \frac{t^2}{2}H_l^2 + i\frac{t^3}{6}H_l^3 + \dots \quad (5)$$

Here we assume that each H_l is a member of the GOE. With the previous expression, it is possible to evaluate the density matrix up to any given order in time in the following way

$$\rho(t) = \frac{1}{N} \sum_l U_l(t) \rho_0 U_l^\dagger(t) = \frac{1}{N} \sum_l \sum_{k=0}^{\infty} \sigma_{l,k} t^k. \quad (6)$$

As we are interested in small values of t , we keep only the first four terms in the expansion (third order in time). These terms are given by

$$\sigma_{l,0} = \rho_0 = |0\rangle\langle 0|, \quad \sigma_{l,1} = i[\rho_0, H_l], \quad (7)$$

$$\sigma_{l,2} = H_l \rho_0 H_l - \frac{1}{2} \{H_l^2, \rho_0\}, \quad (8)$$

$$\sigma_{l,3} = \frac{i}{2} [H_l \rho_0 H_l, H_l] + \frac{i}{6} [H_l^3, \rho_0], \quad (9)$$

where $[H, H']$ and $\{H, H'\}$ respectively stand for the commutator and anticommutator between H and H' . As the GOE is invariant under orthogonal transformations, using a basis state of the Hamiltonian as initial condition is equivalent to choosing a random state with real entries. For this reason, and without loss of generality, we set the initial state to $|\Psi_0\rangle = |0\rangle$, where $|n\rangle$ is a state of the basis where all the random Hamiltonians are constructed and $n = 0, 1, \dots, N-1$. In this way, $\rho_0 = |0\rangle\langle 0|$ represents the density matrix of the initial pure state. We consider terms up to third order in t as it is at this order where the first antisymmetric full matrix appears in $\sigma_{l,3}$, whenever each Hamiltonian H_l is real. From the expressions (7)-(9), one can note that the only terms represented by full matrices are $H_l \rho_0 H_l$, and $[H_l \rho_0 H_l, H_l]$. All other elements contain nonzero entries only in the first column and in the first row. Using this fact, it is possible to separate the terms consisting of full matrices by rewriting the density matrix in the following way

$$\rho(t) \simeq \tilde{\sigma}(t) + \sigma(t). \quad (10)$$

The first term contains only a nonzero element in the first position of the main diagonal. Other $2N-1$ nonzero elements are present in the first column and first row of the matrix, as evidenced by the expression

$$\tilde{\sigma}(t) = |0\rangle\langle 0| + \sum_{n \neq 0} (a_n(t) |0\rangle\langle n| + a_n^*(t) |n\rangle\langle 0|) + \frac{t^2}{2} \mathbb{1}, \quad (11)$$

where $\mathbb{1}$ is the identity matrix and where we have introduced the matrix element

$$a_n(t) = \left(-iH_l t - \frac{1}{2} H_l^2 t^2 + \frac{i}{6} H_l^3 t^3 \right)_{n,0}. \quad (12)$$

The second term in equation (10) is a full matrix, therefore containing N^2 nonzero elements that will dominate the statistics for large N . This term can be written as

$$\sigma(t) = \frac{t^2}{\sqrt{2N}} \left(B + it \frac{\sqrt{N}}{2} D \right), \quad (13)$$

where we have chosen to write it in terms of the real symmetric matrix B and the real antisymmetric matrix D , both with zero mean value and variances given by

$$B_{n,m} = \sqrt{\frac{2}{N}} \sum_{l=1}^N H_{l;n,0} H_{l;0,m} - \sqrt{\frac{N}{2}}, \quad (14)$$

$$D_{n,m} = \frac{\sqrt{2}}{N} \sum_{l=1}^N [(H_l^2)_{n,0} H_{l;0,m} - H_{l;n,0} (H_l^2)_{0,m}]. \quad (15)$$

From the CLT and taking into account the properties of H_l , it is not hard to find that the variances of B and D are given by

$$\langle (B_{n,n})^2 \rangle = 2 \langle (B_{n,m \neq n})^2 \rangle = 2 \langle (D_{n,m \neq n})^2 \rangle = 1. \quad (16)$$

We have considered H_l as an element of the GOE, however, this treatment is also applicable to random symmetric Hamiltonians with zero mean and variances as S in equation (4).

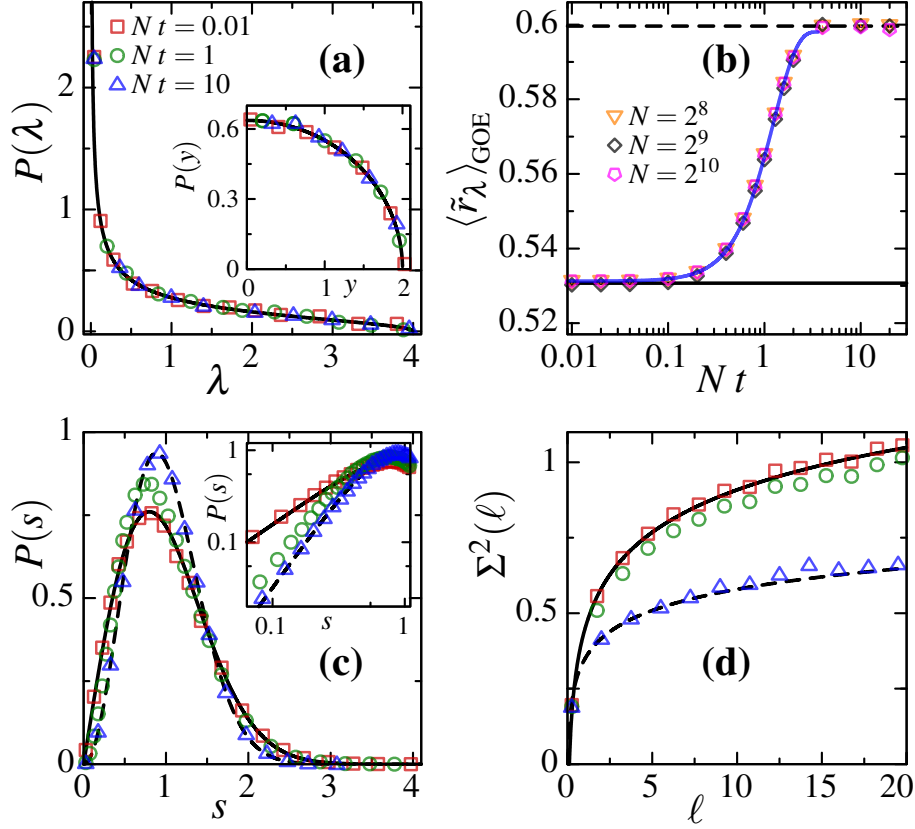


Figure 1. (Color online) (a) Spectral level density of the mixed state compared to the Marchenko-Pastur law of equation (18) in solid line. The inset shows the spectral level density of $y = \sqrt{\lambda}$ compared to the quarter circle law in black line. (b) $\langle \tilde{r}_\lambda \rangle_{\text{GOE}}$ as a function of time rescaled to the system size N . The blue curve corresponds to equation (20) with $a = 0.2832 \pm 0.0021$ and $b = (-4.6210 \pm 0.1857) \times 10^{-3}$. (c) Nearest-neighbor level spacings distribution compared to the Wigner-Dyson surmise, equation (21). A log-log plot is shown in the inset. (d) Level number variance compared to the GOE and GUE expectations as indicated in equation (22). GOE (GUE) predictions are indicated in panels (b)-(d) with solid (dashed) black curves. In (a), (c) and (d) the system size is $N = 2^{10}$, and the different times are indicated in the legend of (a).

By inspection of equation (13), one can realize that the validity of the expansion up to third order in time is restricted to the values of t where the imaginary part of $\sigma(t)$ is much smaller than its real counterpart. This implies the condition $t \ll 2/\sqrt{N}$. GUE statistics should appear in time when this condition is broken. According to the discussion in the previous subsection, the transition should manifest itself in time when the imaginary part of the density matrix is $1/\sqrt{N}$ times smaller than the real part. Therefore, one can conclude that the transition takes place approximately at the time

$$t \sim 2/N. \quad (17)$$

It is important to note that, in contrast with the Hamiltonian in equation (3) for $\alpha = 0$, our density matrix does not belong to the GOE at short times or $t = 0$. However, numerical calculations show GOE-like spectral statistics at short times. For long times, as the density matrix fills up completely with random variables, the correspondence with the GUE becomes a more accurate description. We will show this behavior relying on numerical calculations in the next section.

4 Spectral statistics

In this section we study the statistical properties of the mixed state of equation (2) when the time evolution is generated by an ensemble of Hamiltonians, where each member H_l is taken from the GOE, with $l = 1, \dots, N$. The initial state $|\Psi_0\rangle = (1 \ 0 \ \dots \ 0)^T$, where T stands for the transpose, is chosen from the canonical basis of the Hamiltonian. For the analysis we consider system sizes of $N = 2^n$ with $n = 8, 9$, and 10 , and we perform M random realizations of equation (2) such that the product $N \times M$ remains fixed to $\approx 5 \times 10^5$. Also, for each realization we take only 60% of the eigenvalues around the center of the spectrum. The curve fittings are performed using a nonlinear least-squares fitting. The obtained mixed state can be regarded as the reduced

density matrix of a pure state of a larger composite system. In particular, we show that the distribution of the eigenvalues λ_i , normalized to its standard deviation, converges to the Marchenko-Pastur distribution, which is a characteristic feature of structureless ensembles³. For small times this distribution is only reached by all but one of the eigenvalues, the largest one separated from the bulk.

In Figure 1 (a) we display the spectral level density distribution of the mixed state compared to the Marchenko-Pastur law (continuous line)

$$P(\lambda) = \frac{1}{2\pi} \sqrt{\frac{4}{\lambda} - 1}, \quad \lambda \in [0, 4], \quad (18)$$

for small (red-squares), intermediate (green-circles), and large times (blue-triangles), rescaled to the system size $N = 2^{10}$. As it can be observed, the same behavior is preserved in time. In the inset of the same panel, we show that the level density follows the quarter-circle law, $P(y) = \frac{1}{\pi} \sqrt{4 - y^2}$, in the rescaled variable $y = \sqrt{\lambda}$, characteristic of the so-called Hilbert-Schmidt ensemble of random quantum states⁸.

A further insight about the complexity in the time evolution of the mixed state can be obtained from the average ratio of consecutive eigenvalues spacings, $\langle r \rangle$ or $\langle \tilde{r} \rangle$. These quantities are often used as a measure of the degree of chaoticity of a physical system^{24,25}. We will employ analogue quantities for the eigenvalues of our density matrix. That is, given an ordered set of eigenvalues, $\{\lambda_i\}$, the nearest neighbor spacings are $\Delta_i = \lambda_{i+1} - \lambda_i$ and the ratio of consecutive eigenvalues spacings, r_i , and \tilde{r}_i are defined as

$$r_i = \frac{\Delta_i}{\Delta_{i-1}} \quad \text{and} \quad \tilde{r}_i = \min\left(r_i, \frac{1}{r_i}\right). \quad (19)$$

Furthermore, the dynamical behavior of the average value $\langle \tilde{r} \rangle$ as a function of the parameter $\tau \in [0, 1]$ is given by²⁶

$$\begin{aligned} \langle \tilde{r}(\tau) \rangle = & \frac{4(2 + \tau^2)}{\pi(1 - \tau^2)} \arctan\left[\frac{\sqrt{3}(1 + \tau^2)}{2\tau}\right] - \frac{4\sqrt{3}}{\pi(1 - \tau^2)^{3/2}} \arctan\left[\frac{(1 - \tau^2)^{3/2}}{\tau(3 + \tau^2)}\right] - \frac{17 + 7\tau^2}{\pi(1 - \tau^2)} \arctan\left(\frac{\tau}{\sqrt{3}}\right) \\ & - \frac{1}{\pi} \arctan(\sqrt{3}\tau). \end{aligned} \quad (20)$$

This expression, derived in a Hamiltonian context, describes the crossover from GOE to GUE. Here we will show that it also describes the crossover of the ensemble of density matrices introduced in Sec. 2. In this case $\tau \rightarrow Nt$ plus a shift due to the rescaling in time. For sake of clarity, we include a subscript λ in $\langle \tilde{r}_\lambda \rangle_{\text{GOE}}$ to indicate that this quantity is calculated from the eigenvalues $\{\lambda_i\}$ of the density matrix in equation (2).

In Figure 1 (b), we show $\langle \tilde{r}_\lambda \rangle_{\text{GOE}}$ as function of Nt for system sizes $N = 2^n$ with $n = 8, 9$, and 10 , in orange inverted-triangles, black diamonds, and magenta pentagons, respectively. The black horizontal lines correspond to RMT prediction fittings, $\langle \tilde{r} \rangle_{\text{GOE}}^{\text{fit}} \approx 0.5307$ (continuous) and $\langle \tilde{r} \rangle_{\text{GUE}}^{\text{fit}} \approx 0.5996$ (dashed), for the GOE and GUE respectively²⁵. For small times, $\langle \tilde{r}_\lambda \rangle_{\text{GOE}}$ agrees with RMT predictions for the GOE and with our short-time dynamics analysis in Sec. 3.1. For intermediate times and in accordance with equation (17), the eigenvalue statistics departs from GOE and completely reaches GUE at times $t \approx 2/N$. This transition is analog to the transition from GOE to GUE that occurs in Hamiltonian systems when time reversal symmetry is broken by a magnetic field. Here, however, the transition does not have to do with the breaking of time-reversal symmetry, but with the number of statistically independent elements in the mixed state, which is $N(N-1)/2$ for the GOE and $N(N-1)$ for the GUE. For short times we have $N' = N^2 - 2N + 1$ real elements. Finally, the blue continuous line corresponds to $\langle \tilde{r}(a\tau) \rangle + b$, where $\langle \tilde{r}(\tau) \rangle$ is given by equation (20) and a and b are fitting parameters. Here, $a = 0.2832 \pm 0.0021$ and $b = (-4.6210 \pm 0.1857) \times 10^{-3}$ are the best fittings to the numerical data in the range of validity $0 \leq Nt \leq 1/a$.

Now, in order to characterize the spectral level density, we use the Wigner-Dyson nearest-neighbor level spacing distribution and the level number variance. On one hand, the Wigner-Dyson distribution characterizes the short-range correlations of the spectrum and is usually used as an indicator of the chaoticity of a given physical system. To a good approximation, it is given by the so-called Wigner surmise²⁷

$$P_{\text{WD}}(s) = \begin{cases} \frac{\pi}{2} s \exp\left(-\frac{\pi}{4} s^2\right) & \text{for GOE,} \\ \frac{32}{\pi^2} s^2 \exp\left(-\frac{4}{\pi} s^2\right) & \text{for GUE.} \end{cases} \quad (21)$$

In equation (21), $s = \Delta_i / \langle \Delta \rangle$ being $\langle \Delta \rangle$ the mean level spacing. On the other hand, the long-range level correlations are characterized through the level number variance, or the variance of the number of unfolded eigenvalues in an interval of length

ℓ , namely

$$\Sigma^2(\ell) \approx \begin{cases} \frac{2}{\pi^2} \left[\log(2\pi\ell) + \gamma + 1 - \frac{\pi^2}{8} \right] & \text{for GOE,} \\ \frac{1}{\pi^2} \left[\log(2\pi\ell) + \gamma + 1 \right] & \text{for GUE,} \end{cases} \quad (22)$$

where $\gamma \approx 0.577 \dots$ is the Euler constant. In order to separate the universal from the non-universal behavior in the spectral density, we first perform the unfolding procedure that yields to a spectral level density in which the mean level spacing is equal to unity²⁷. Here, the unfolding is done by employing a seventh degree polynomial.

In Figure 1 (c), we show the nearest-neighbor level spacing distribution, $P(s)$, of the mixed state for a system size $N = 2^{10}$, for small (red-squares), intermediate (green-circles), and large times (blue-triangles): $Nt = 0.01$, $Nt = 1$, and $Nt = 10$, respectively. The black curves correspond to the Wigner-Dyson surmise of equation (21) for the GOE (continuous) and the GUE (dashed) cases. As it is observed, for small and large times these statistics are in agreement with the Wigner surmise for the GOE and GUE cases, respectively. This is in accordance with the behavior observed in panel (b) of the same figure. Furthermore, for intermediate times the distribution is neither GOE nor GUE, but a distribution in between both statistics. Also, let us notice that for small level spacings, s , the degree of level repulsion increases smoothly from linear to quadratic, or from GOE to GUE, as the system evolves in time without the presence of any magnetic field, as usually happens in Hamiltonian systems in RMT. In the inset of the same panel, this transition in a log-log plot is shown. In panel (d) of the same figure, we display the long-range correlations of the spectra, characterized by the level number variance [see equation (22)], for the three mentioned times. Again, the transition from GOE to GUE is clearly observed.

5 Evolution under interacting spin-1/2 Hamiltonians

This section is devoted to corroborate our previous results based on RMT in a more realistic context, that is, we show that the transition with time to the GUE distribution also occurs when the dynamics of the density matrix in equation (1) is dictated by the Hamiltonian

$$H = \sum_{k=1}^L (S_k^x S_{k+1}^x + S_k^y S_{k+1}^y + S_k^z S_{k+1}^z) + \sum_{k=1}^L h_k S_k^z. \quad (23)$$

This Hamiltonian describes a one-dimensional system of spin-1/2 particles interacting between nearest neighbors, each particle is located in one of the L sites of a chain and subject to an on-site disordered magnetic field. It has become paradigmatic in studies of the so-called many-body localization (MBL) transition/crossover^{28–30}. In Hamiltonian (23) $\hbar = 1$, $S_k^{x,y,z}$ are spin-1/2 operators acting on site k and h_k are random numbers from a flat distribution in the interval $(-h, h)$, with h being the disorder strength. Additionally, periodic boundary conditions are assumed, $S_{L+1}^{x,y,x} = S_1^{x,y,x}$. The Hilbert space dimension is $\dim(\mathcal{H}) = 2^L$, but since the total magnetization in z -direction $\mathcal{S}^z = \sum_{k=1}^L S_k^z$ is conserved, the whole space splits in $L+1$ subspaces, each one corresponding to a fixed value of \mathcal{S}^z and of size $N = L!/[N_{\text{up}}!(L-N_{\text{up}})!]$, with N_{up} the number of spins up or excitations contained in each subspace. We concentrate our analysis on two subspaces, namely in the half-filling subspace where $N_{\text{up}} = L/2$ and in the one-excitation subspace where $N_{\text{up}} = 1$.

For a fair comparison with our GOE results, we ensure that the system described by equation (23) is in the chaotic regime, meaning that its energy levels are correlated in a similar way as the eigenvalues of GOE matrices^{31,32}. We fix $h = 0.5$ for the half-filling subspace and $h = 0.1$ for the one-excitation subspace. Previously, we mentioned that our choice of initial state in the RMT case was equivalent to a random real state. In this section we start from a random real state, as the Hamiltonian in equation (23) is not invariant under orthogonal transformations. Therefore, in both cases the initial state is a pure state whose components are real random variables following a Gaussian distribution with mean zero and variance one.

5.1 Half filling subspace

The half-filling (HF) subspace corresponds to $\mathcal{S}^z = 0$ which leads to $N = L!/(L/2)!^2$. For our analysis we set $L = 12$; therefore, $N = 924$. As stated in Sec. 2, we perform $M = 541$ realizations in equation (2) so that for the spectral statistics we count with almost 5×10^5 eigenvalues.

It is worth to mention that when simulating the dynamics in the half-filling subspace we realized that for short times, $t \ll 1$, many eigenvalues were $\leq 10^{-15}$, then it was necessary to impose a restriction over the eigenvalues to be considered in our statistical analysis, thus avoiding possible numerical machine precision errors. In particular, we consider the spectrum $\{\lambda_i\}$ in increasing order and take only the first \mathcal{N} eigenvalues such that $\sum_i^{\mathcal{N}} \lambda_i = 0.99 \dots 9$ up to twelve significant figures. We found that $\mathcal{N} \ll N$ for small times and usually $\mathcal{N} = N$ for $t \gtrsim 0.1$.

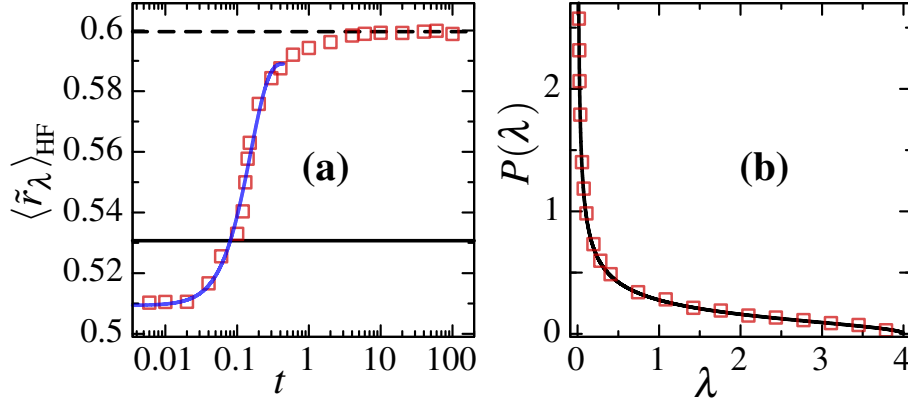


Figure 2. (Color online) Spectral statistics of the density matrix ensemble (2) when the time evolution is dictated by an ensemble of Hamiltonians taken from the spin-1/2 model (23) in the HF subspace with $h = 0.5$. **(a)** $\langle \tilde{r}_\lambda \rangle_{\text{HF}}$ as a function of time (red squares). Black solid (dashed) line is the $\langle \tilde{r} \rangle_{\text{GOE}}^{\text{fit}}$ ($\langle \tilde{r} \rangle_{\text{GUE}}^{\text{fit}}$). The blue solid curve corresponds to the best fitting using equation (20) via $\langle \tilde{r}(at) \rangle c + b$ with $a = 2.2661 \pm 0.1117$, $b = -0.1296 \pm 0.02297$ and $c = 1.1924 \pm 0.04107$. **(b)** Spectral level density $P(\lambda)$ for $t = 100$ (red squares) compared to the Marchenko-Pastur law given by equation (18) (black curve). System size is $L = 12$ ($N = 924$).

Figure 2 (a) depicts $\langle \tilde{r}_\lambda \rangle_{\text{HF}}$ in the HF subspace as a function of time t . The first thing to note is that the universal transition to GUE statistics also occurs in this case, i.e., for large times $\langle \tilde{r}_\lambda \rangle_{\text{HF}}$ (red squares) $\rightarrow \langle \tilde{r} \rangle_{\text{GUE}}^{\text{fit}}$ (black dashed line); however, in contrast with the case when the dynamics is dictated by GOE matrices, the starting value of $\langle \tilde{r}_\lambda \rangle_{\text{HF}}$ does not coincide with $\langle \tilde{r} \rangle_{\text{GOE}}^{\text{fit}}$ (black solid line). Specifically, for $t \lesssim 0.02$ we observe $\langle \tilde{r}_\lambda \rangle_{\text{HF}} \approx 0.51 < \langle \tilde{r} \rangle_{\text{GOE}}^{\text{fit}}$, meaning that the correlations between eigenvalues of the density matrix evolved with Hamiltonians with the form given by equation (23) are weaker than those from the density matrix evolved with GOE matrices, $\langle \tilde{r} \rangle_{\text{GOE}}^{\text{fit}}$. After the initial plateau, $\langle \tilde{r}_\lambda \rangle_{\text{HF}}$ shows a transient increasing within the time interval $0.02 \lesssim t \lesssim 5$. Finally, when the time is large enough, $t \gtrsim 5$, the statistics reach and remain in the $\langle \tilde{r} \rangle_{\text{GUE}}^{\text{fit}}$ value. In Figure 2 (a) we also include a blue solid curve representing a fitting obtained via the function $\langle \tilde{r}(at) \rangle c + b$, where $\langle \tilde{r}(t) \rangle$ is given by equation (20), with a, b and c being fitting parameters. We found the values $a = 2.2661 \pm 0.1117$, $b = -0.1296 \pm 0.02297$ and $c = 1.1924 \pm 0.04107$ in the range of validity $0 \leq t \leq 0.34$.

The lack of agreement between $\langle \tilde{r}_\lambda \rangle_{\text{HF}}$ and $\langle \tilde{r} \rangle_{\text{GOE}}^{\text{fit}}$ at the short-time scale is explained as follows. Since at half-filling the Hamiltonian (23) contains only L statistically independent random variables, a number which is in general much smaller than N , the CLT cannot be applied to equations (14) and (15); thus, the elements of matrices B and D in Eq (13) cannot be taken as uncorrelated Gaussian random variables. In order to reinforce our previous arguments we will show in the next subsection that an enough number of independent random variables in Hamiltonian (23) leads to initial eigenvalues statistics that agree with $\langle \tilde{r} \rangle_{\text{GOE}}^{\text{fit}}$.

Before that, let us complete our analysis by studying the distribution $P(\lambda)$ for the eigenvalues λ_i of the density matrix ensemble in the HF subspace. In Figure 2 (b) we display the distribution $P(\lambda)$ at time $t = 100$ (red squares), it shows a very good agreement with the Marchenko-Pastur distribution given in equation (18) (black line). However, this agreement is only observed for times $t \gtrsim 20$ and where, as already discussed, $\langle \tilde{r}_\lambda \rangle_{\text{HF}}$ coincides with the GUE statistics. For short times (not shown) $P(\lambda)$ is far from the Marchenko-Pastur distribution. Therefore, we can ensure that only at large times the density matrix generated according to equation (2) and evolved with Hamiltonian equation (23) in the HF subspace can be considered as a genuine random density matrix from a Hilbert-Schmidt ensemble. This marks another important difference with the density matrix evolved with GOE matrices, for which the distribution $P(\lambda)$ agrees very well with the Marchenko-Pastur distribution from short to large times [see Figure 1 (a)].

5.2 One excitation subspace

In this section we repeat the analysis done in Subsec. 5.1 for a density matrix which is evolved under Hamiltonians with the form given in equation (23), but now in the subspace where only one excitation (OE) is present in the chain. The dimension of this subspace is $N = L$, a convenient fact for our purposes because in this case the number of statistically independent random variables in the Hamiltonian equals the dimension of the subspace. We set $L = 924$ and $M = 541$, and remind that for the OE subspace we fix the disorder strength in equation (23), $h = 0.1$. The initial state is the same one used for the analysis in the HF subspace.

Figure 3 (a) shows our numerical results for the dynamical statistical behavior of $\langle \tilde{r}_\lambda \rangle_{\text{OE}}$ (red squares). We observe that

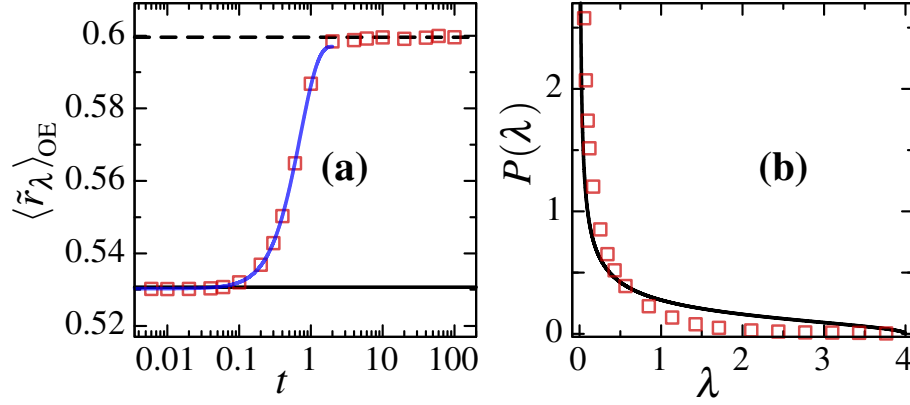


Figure 3. (Color online) Spectral statistics of the density matrix ensemble (2) when the time evolution is dictated by an ensemble of Hamiltonians taken from the spin-1/2 model (23) in the OE subspace with $h = 0.1$. **(a)** $\langle \tilde{r}_\lambda \rangle_{\text{OE}}$ as a function of time (red squares). Black solid (dashed) line is the $\langle \tilde{r} \rangle_{\text{GOE}}^{\text{fit}}$ ($\langle \tilde{r} \rangle_{\text{GUE}}^{\text{fit}}$). The blue solid curve corresponds to the best fitting using equation (20) via $\langle \tilde{r}(at) \rangle + b$, with $a = 0.4900 \pm 0.0024$ and $b = -0.0056 \pm 6.8 \times 10^{-5}$. **(b)** Spectral level density $P(\lambda)$ for $t = 100$ (red squares) compared to the Marchenko-Pastur law given by equation (18) (black curve). System size is $L = 924$ ($N = 924$).

$\langle \tilde{r}_\lambda \rangle_{\text{OE}}$ agrees for short times with $\langle \tilde{r} \rangle_{\text{GOE}}^{\text{fit}}$ (black solid line), while for large times there is an agreement with $\langle \tilde{r} \rangle_{\text{GUE}}^{\text{fit}}$ (black dashed line). This is a remarkable qualitative correspondence with the behavior of $\langle \tilde{r}_\lambda \rangle_{\text{GOE}}$ [see Figure 1 (b)]. Furthermore, $\langle \tilde{r}_\lambda \rangle_{\text{OE}}$ is well described by equation (20) via the fitting $\langle \tilde{r}(at) \rangle + b$ (blue solid curve), with $a = 0.4900 \pm 0.0024$ and $b = -0.0056 \pm 6.8 \times 10^{-5}$, and in the validity range $0 \leq t \lesssim 2$.

For completeness, we show in Figure 3 (b) the distribution $P(\lambda)$ for the eigenvalues of the density matrix, but now evolved in the OE subspace (red squares). The time is again large, $t = 100$, but in this case the Marchenko-Pastur distribution (black curve) is not reached. At first glance this could be surprising, specially because at this time scale $\langle \tilde{r}_\lambda \rangle_{\text{OE}}$ already coincides with $\langle \tilde{r} \rangle_{\text{GUE}}^{\text{fit}}$, however, Hamiltonian (23) with one excitation is equivalent to a system without interactions and at this level, differences between models with and without interactions are well known, an example is their density of states^{33–35}.

In addition to the previous discussion, let us note that for the corresponding disorder strength h used in each case, HF ($h = 0.5$) and OE ($h = 0.1$) subspaces, the level spacing distribution of Hamiltonian (23) is GOE-like; however, there is an essential distinction between both cases, related to the presence or absence of interactions, namely for the HF subspace an infinitesimal disorder strength could bring the system to a chaotic regime in the thermodynamic limit ($L \rightarrow \infty$)³⁶, meanwhile for the OE subspace in the same limit, an infinitesimal disorder strength will induce single-particle-like localization and the level spacing distribution will be the corresponding to uncorrelated random variables from a Poisson process^{37,38}. Interestingly, this fact could be indicating that the distribution $P(\lambda)$ of eigenvalues of the random density matrix (2) is more sensitive for the characterization of the chaotic nature of a given finite system than the level spacing distribution of the associated Hamiltonian. But this last point needs further studies.

Above all, in this subsection we have validated that the number of statistically independent real random variables needed in order to have a crossover from GOE to the universal GUE in the statistics of the eigenvalues of the density matrix generated according to equation (2) should be at least $\mathcal{O}(N)$.

6 Conclusions

In this paper, we have studied the time dynamics of random density matrices generated by evolving a pure state using two different ensembles of random Hamiltonians. In the first case, we consider an ensemble of Hamiltonians that belong to the GOE and showed that the resulting ensemble of mixed states undergoes a crossover from the GOE to the GUE in their spectral statistics. This crossover occurs in a time scale that depends on the system size and is explained in terms of the elements of the density matrix, which are real or complex uncorrelated Gaussian random variables for short and large times, respectively.

In the second case, we showed that the GOE to GUE crossover is also present in more realistic contexts. Here, the time evolution of the ensemble of mixed states is dictated by an ensemble of spin-1/2 Hamiltonians including on-site disorder and displaying GOE statistics. Particularly, two subsectors of the Hamiltonians are considered: one with interactions between the particles and another one that due to its single excitation nature can be considered as without interactions. For these cases the spectral statistics of the generated mixed state shows, at short times, a strong dependence on the number of statistically independent random variables present in the Hamiltonians. Furthermore, at large times, even though both ensembles of mixed

states reach their final universal form, marked by GUE statistics, only the mixed states generated by the ensemble of spin-1/2 Hamiltonians, in the subspace that takes interactions into account, lead to genuine random density matrices that belong to the Hilbert-Schmidt ensemble, whose level density follows a Marchenko-Pastur distribution.

In general such a crossover is not always present. For instance, using complex random Hamiltonians to generate the evolution, the eigenvalues statistics of the density matrix will resemble the GUE for all times. In contrast, using antisymmetric Hamiltonians will lead to a constant GOE behavior. We emphasize, however, that for real Hamiltonians with random components the crossover to GUE statistics studied here marks the onset of universality of dynamically generated random density matrices.

It would be interesting to study further statistical properties of random density matrices, such as the time dependence of the eigenstates structure, together with the distribution of their components. Additional studies on the eigenvalues distribution could assist in chaos detection in different Hamiltonian scenarios.

References

1. Wootters, W. K. Random quantum states. *Found. Phys.* **20**, 1365, DOI: [10.1007/BF01883491](https://doi.org/10.1007/BF01883491) (1990).
2. Collins, B. & Nechita, I. Random matrix techniques in quantum information theory. *J. Math. Phys.* **57**, 015215, DOI: [10.1063/1.4936880](https://doi.org/10.1063/1.4936880) (2016).
3. Życzkowski, K., Penson, K. A., Nechita, I. & Collins, B. Generating random density matrices. *J. Math. Phys.* **52**, 062201, DOI: [10.1063/1.3595693](https://doi.org/10.1063/1.3595693) (2011).
4. Pineda, C. & Seligman, H. T. Random density matrices versus random evolution of open system. *J. Phys. A: Math. Theor.* **48**, 425005, DOI: [10.1088/1751-8113/48/42/425005](https://doi.org/10.1088/1751-8113/48/42/425005) (2015).
5. Chamon, C., Hamma, A. & Mucciolo, E. R. Emergent irreversibility and entanglement spectrum statistics. *Phys. Rev. Lett.* **112**, 240501, DOI: [10.1103/PhysRevLett.112.240501](https://doi.org/10.1103/PhysRevLett.112.240501) (2014).
6. Yang, Z.-C., Hamma, A., Giampaolo, S. M., Mucciolo, E. R. & Chamon, C. Entanglement complexity in quantum many-body dynamics, thermalization, and localization. *Phys. Rev. B* **96**, 020408, DOI: [10.1103/PhysRevB.96.020408](https://doi.org/10.1103/PhysRevB.96.020408) (2017).
7. Sarkar, A. & Kumar, S. Generation of bures-hall mixed states using coupled kicked tops. *Phys. Rev. A* **103**, 032423, DOI: [10.1103/PhysRevA.103.032423](https://doi.org/10.1103/PhysRevA.103.032423) (2021).
8. Sommers, H.-J. & Życzkowski, K. Statistical properties of random density matrices. *J. Phys. A: Math. Gen.* **37**, 8457, DOI: [10.1088/0305-4470/37/35/004](https://doi.org/10.1088/0305-4470/37/35/004) (2004).
9. Žnidarič, M. Entanglement of random vectors. *J. Phys. A: Math. Theor.* **40**, F105, DOI: [10.1088/1751-8113/40/3/f04](https://doi.org/10.1088/1751-8113/40/3/f04) (2007).
10. Bassler, K. E., Forrester, P. J. & Frankel, N. E. Eigenvalue separation in some random matrix models. *J. Math. Phys.* **50**, 033302, DOI: [10.1063/1.3081391](https://doi.org/10.1063/1.3081391) (2009).
11. Pandey, A. & Mehta, M. Gaussian ensembles of random hermitian matrices intermediate between orthogonal and unitary ones. *Commun. Math. Phys.* **87**, 449–468, DOI: [10.1007/BF01208259](https://doi.org/10.1007/BF01208259) (1983).
12. Schierenberg, S., Bruckmann, F. & Wettig, T. Wigner surmise for mixed symmetry classes in random matrix theory. *Phys. Rev. E* **85**, 061130, DOI: [10.1103/PhysRevE.85.061130](https://doi.org/10.1103/PhysRevE.85.061130) (2012).
13. Lenz, G. & Haake, F. Reliability of small matrices for large spectra with nonuniversal fluctuations. *Phys. Rev. Lett.* **67**, 1, DOI: [10.1103/PhysRevLett.67.1](https://doi.org/10.1103/PhysRevLett.67.1) (1991).
14. Schweiner, F., Main, J. & Wunner, G. GOE-GUE-poisson transitions in the nearest-neighbor spacing distribution of magnetoexcitons. *Phys. Rev. E* **95**, 062205, DOI: [10.1103/PhysRevE.95.062205](https://doi.org/10.1103/PhysRevE.95.062205) (2017).
15. So, P., Anlage, M. S., Ott, E. & Oerter, R. N. Wave chaos experiments with and without time reversal symmetry: GUE and GOE statistics. *Phys. Rev. Lett.* **74**, 2662, DOI: [10.1103/PhysRevLett.74.2662](https://doi.org/10.1103/PhysRevLett.74.2662) (1995).
16. Schäfer, R. *et al.* Transition from gaussian-orthogonal to gaussian-unitary ensemble in a microwave billiard with threefold symmetry. *Phys. Rev. E* **66**, 016202, DOI: [10.1103/PhysRevE.66.016202](https://doi.org/10.1103/PhysRevE.66.016202) (2002).
17. Haake, F., Kuś, M. & Scharf, R. Classical and quantum chaos for a kicked top. *Z. Phys. B Condens. Matter* **65**, 381–395, DOI: [10.1007/BF01303727](https://doi.org/10.1007/BF01303727) (1987).
18. Mierzejewski, M., Prosen, T., Crivelli, D. & Prelovšek, P. Eigenvalue statistics of reduced density matrix during driving and relaxation. *Phys. Rev. Lett.* **110**, 200602, DOI: [10.1103/PhysRevLett.110.200602](https://doi.org/10.1103/PhysRevLett.110.200602) (2013).

19. Beenakker, C. W. J. Random-matrix theory of quantum transport. *Rev. Mod. Phys.* **69**, 731–808, DOI: [10.1103/RevModPhys.69.731](https://doi.org/10.1103/RevModPhys.69.731) (1997).
20. Aßmann, M., Thewes, J., Fröhlich, D. & Bayer, M. Quantum chaos and breaking of all anti-unitary symmetries in rydberg excitons. *Nat. Mater.* **15**, 741–745, DOI: [10.1038/nmat4622](https://doi.org/10.1038/nmat4622) (2016).
21. Schweiner, F., Main, J. & Wunner, G. Magnetoexcitons break antiunitary symmetries. *Phys. Rev. Lett.* **118**, 046401, DOI: [10.1103/PhysRevLett.118.046401](https://doi.org/10.1103/PhysRevLett.118.046401) (2017).
22. Mehta, M. L. & Pandey, A. On some gaussian ensembles of hermitian matrices. *J. Phys. A: Math. Gen.* **16**, 2655–2684, DOI: [10.1088/0305-4470/16/12/014](https://doi.org/10.1088/0305-4470/16/12/014) (1983).
23. Kanazawa, T. Unitary matrix integral for QCD with real quarks and the GOE-GUE crossover. *Phys. Rev. D* **102**, 034036, DOI: [10.1103/PhysRevD.102.034036](https://doi.org/10.1103/PhysRevD.102.034036) (2020).
24. Oganessian, V. & Huse, D. A. Localization of interacting fermions at high temperature. *Phys. Rev. B* **75**, 155111, DOI: [10.1103/PhysRevB.75.155111](https://doi.org/10.1103/PhysRevB.75.155111) (2007).
25. Atas, Y. Y., Bogomolny, E., Giraud, O. & Roux, G. Distribution of the ratio of consecutive level spacings in random matrix ensembles. *Phys. Rev. Lett.* **110**, 084101, DOI: [10.1103/PhysRevLett.110.084101](https://doi.org/10.1103/PhysRevLett.110.084101) (2013).
26. Sarkar, A., Kothiyal, M. & Kumar, S. Distribution of the ratio of two consecutive level spacings in orthogonal to unitary crossover ensembles. *Phys. Rev. E* **101**, 012216, DOI: [10.1103/PhysRevE.101.012216](https://doi.org/10.1103/PhysRevE.101.012216) (2020).
27. Mehta, M. L. *Random Matrices and the Statistical Theory of Energy Levels* (Academic Press, New York, 2004).
28. Pal, A. & Huse, D. A. Many-body localization phase transition. *Phys. Rev. B* **82**, 174411, DOI: [10.1103/PhysRevB.82.174411](https://doi.org/10.1103/PhysRevB.82.174411) (2010).
29. Abanin, D. A. & Papić, Z. Recent progress in many-body localization. *Ann. Phys.* **529**, 1700169, DOI: [10.1002/andp.201700169](https://doi.org/10.1002/andp.201700169) (2017).
30. Alet, F. & Laflorencie, N. Many-body localization: An introduction and selected topics. *C. R. Phys.* **19**, 498, DOI: [10.1016/j.crhy.2018.03.003](https://doi.org/10.1016/j.crhy.2018.03.003) (2018).
31. Torres-Herrera, E. J. & Santos, L. F. Extended nonergodic states in disordered many-body quantum systems. *Ann. Phys. (Berlin)* **529**, 1600284, DOI: [10.1002/andp.201600284](https://doi.org/10.1002/andp.201600284) (2017).
32. Torres-Herrera, E. J. & Santos, L. F. Signatures of chaos and thermalization in the dynamics of many-body quantum systems. *Eur. Phys. J. Spec. Top.* **227**, 1897, DOI: [10.1140/epjst/e2019-800057-8](https://doi.org/10.1140/epjst/e2019-800057-8) (2019).
33. French, J. & Wong, S. Validity of random matrix theories for many-particle systems. *Phys. Lett. B* **33**, 449–452, DOI: [10.1016/0370-2693\(70\)90213-3](https://doi.org/10.1016/0370-2693(70)90213-3) (1970).
34. Schiulaz, M., Távora, M. & Santos, L. F. From few-to many-body quantum systems. *Quantum Sci. Technol.* **3**, 044006, DOI: [10.1088/2058-9565/aad913](https://doi.org/10.1088/2058-9565/aad913) (2018).
35. Zisling, G., Santos, L. F. & Lev, Y. B. How many particles make up a chaotic many-body quantum system. *SciPost Phys.* **10**, 88, DOI: [10.21468/SciPostPhys.10.4.088](https://doi.org/10.21468/SciPostPhys.10.4.088) (2021).
36. Santos, L. F., Pérez-Bernal, F. & Torres-Herrera, E. J. Speck of chaos. *Phys. Rev. Res.* **2**, 043034, DOI: [10.1103/PhysRevResearch.2.043034](https://doi.org/10.1103/PhysRevResearch.2.043034) (2020).
37. Sorathia, S., Izrailev, F., Zelevinsky, V. & Celardo, G. From closed to open one-dimensional anderson model: Transport versus spectral statistics. *Phys. Rev. E* **86**, 011142, DOI: [10.1103/PhysRevE.86.011142](https://doi.org/10.1103/PhysRevE.86.011142) (2012).
38. Torres-Herrera, E. J., Méndez-Bermúdez, J. & Santos, L. F. Level repulsion and dynamics in the finite one-dimensional anderson model. *Phys. Rev. E* **100**, 022142, DOI: [10.1103/PhysRevE.100.022142](https://doi.org/10.1103/PhysRevE.100.022142) (2019).

Acknowledgements

E.J.T.-H., and J.M.T. are grateful for financial support from Proyectos VIEP 2021, BUAP, project number 100524481-VIEP2021. J.M.T. also acknowledges support from the project number 100527172-VIEP2021.